ANL/NE-18/2

Argonne NATIONAL LABORATORY

Generation of the Cross Section Library for PROTEUS

Nuclear Engineering Division

ANL/NE-18/2

Generation of the Cross Section Library for PROTEUS

prepared by

Changho Lee and Yeon Sang Jung
Nuclear Engineering Division, Argonne National Laboratory

January 30, 2018

ABSTRACT

The cross sections for a high-fidelity neutron transport code PROTEUS can be generated in multiple ways. Multigroup cross sections in the ISOTXS format can be generated using the external codes such as MC^2-3 and Monte Carlo codes such as Serpent and OpenMC. For the Monte Carlo codes, their multigroup cross section outputs should be converted to the ISOTXS format using a post processor named GenISOTXS developed by ANL. In addition, multigroup cross sections can be generated on the fly using the cross section API in PROTEUS along with the cross section library. Currently, the cross section API implemented in PROTEUS includes two cross section method options: the subgroup method and the resonance table method, both of which require the fixed source calculations at each energy group. Recently, the cross section library of PROTEUS has been updated based on the resonance table method with the 41-group structure, for which the base isotopic cross sections were generated using the OpenMC Monte Carlo code and the corresponding background cross sections were calculated using the MC^2-3 code with its 2-D MOC capability, based on a unit pin cell with various background cross section conditions of each isotope. This report focuses on describing the new cross section library and its performance. Verification tests were also conducted with the Mosteller pin cell benchmarks, the VERA fuel assemblies, and the modified C5 core benchmark problems. The results with the new cross section library indicated that eigenvalues, pin power distributions, and temperature coefficients from PROTEUS were in very good agreement with corresponding Monte Carlo solutions.

TABLE OF CONTENTS

LIST OF FIGURES

LIST OF TABLES

1. Introduction

The PROTEUS [1,2] code, developed by Argonne national laboratory (ANL) under the U.S. DOE NEAMS program, is a high fidelity neutron transport code based on unstructured finite element meshes, which is a main component of the SHARP high-fidelity multi-physics simulation package [2]. Three method options are available in the latest version of PROTEUS: the 2nd-order discrete ordinate method (SN2ND), the method of characteristics (MOC), and the nodal transport method (NODAL) which was recently implemented. For MOC, the two-dimensional (2-D) MOC with a discontinuous Galerkin finite element method in the axial direction based on a 2-D extruded geometry (named MOCEX) [2], in addition to a traditional 3-D MOC (named MOCFE), is being used as a main MOC solver because of its better performance in terms of computational time and resources than MOCFE.

Multigroup cross sections are one of the key elements to determine the accuracy of deterministic neutronics codes. For PROTEUS multigroup cross sections can be provided from external codes in the ISOTXS format or generated using the cross section application programming interface (CSAPI) [3] on the fly inside the code. The CSAPI was developed to easily facilitate the use of the developed cross section libraries into existing neutron transport codes and to provide a convenient and flexible framework to implement versatile cross section methods. In order to use the CSAPI, a transport code must provide it with a fixed-source transport solver, a mapping of compositions to the physical domain, and the configuration of cross section regions. The CSAPI currently supports two cross section method options: the subgroup method [5] and the resonance table method [4].

Previously, an attempt was made to develop a generalized cross section library that is able to deal with applications with a wide range of spectrum. [3] For the wide range of applications, a base ultrafine group (UFG > 2100 groups) cross section library was generated using MC^2-3 [6] and NJOY 7], which includes resonance cross section tables as a function of background cross section and temperature for each isotope. A group condensation optimization algorithm was used to condense the UFG library to a broad group (BG) library that is actually used in PROTEUS for a particular reactor or a reactor type of interest. However, this approach has some drawbacks in its practical use in that the size of the base cross section library is too large and high-fidelity deterministic codes like PROTEUS actually needs as small cross section library as possible to reduce their computation time and resources, maintaining good solution accuracy.

Last year, we updated the microscopic cross section generation process of OpenMC [7], developing the GenISOTXS code [9] that processes the cross section outputs from Serpent [10] and OpenMC to produce a cross section file in the ISOTXS format and verifying that the isotopic cross sections tallied from OpenMC worked well for small benchmark problems. [9] The isotopic cross sections generated using OpenMC (or any Monte Carlo codes that are able to generate a complete set of microscopic cross sections) with heterogeneous pin cells based on the reactor or reactor type of interest as long as resonance cross sections can be accurately estimated as a function of the background cross sections in a consistent manner both when preparing the cross section library and solving reactor problems. This will minimize the sources of differences in cross sections between deterministic and Monte Carlo approaches and make us easier to resolve any discrepancies in verification tests in which deterministic solutions are normally compared with Monte Carlo solutions.

In this report, the cross section methodologies that PROTEUS can use are discussed in Section 2. Detailed descriptions on the cross section library generation are given in Section 3, focusing on the recent approach with the OpenMC and MC^2-3 codes. Verification test results are presented in Section 4. Conclusions are provided in Section 5.

2. Multigroup Cross Sections for PROTEUS

The PROTEUS code is able to read multigroup cross sections in the ISOTXS format provided offline using cross section generation codes or to generate multigroup cross sections on the fly using the cross section library which includes isotropic cross sections and resonance parameters as a function of temperature and background cross section. For the latter, the cross section application programing interface (CSAPI) was developed to make it easy to plug the developed cross section module into an existing neutron transport code.

The CSAPI in PROTEUS is composed of largely several modules of reading the cross section library, solving the fixed source problems, interpolating cross sections using temperature and background cross section, and constructing and assigning multigroup cross sections for use in PROTEUS. The CSAPI calculates multigroup cross sections for every cross section region of a problem (pin, assembly, or core) of interest, accounting for temperature and energy and spatial resonance self-shielding conditions. The CSAPI currently includes two cross section methodology options: the subgroup method and the resonance table method. Both the methods require the fixed source calculations at each energy group.

2.1 Multigroup Cross Sections in the ISOTXS format

2.1.1 Using MC^2-3

The MC^2-3 code is a well-known multigroup cross section generation code developed initially for fast reactor systems. Recently, its thermal cross section library was extended down to 10^{-5} eV to fully cover thermal energy neutrons. Up-scattering and S(α,β) cross sections were included in the cross section library as well. Two thermal cross section options are currently available: the broad group option based on the Dancoff approach [11] (43 energy groups below 10 eV) and the almost pointwise cross section option [12] (1,700 energy groups below 4 eV).

In addition, 2-D and 3-D MOC capabilities were implemented for Cartesian and hexagonal geometries, based on the same MOC methodology as PROTEUS, so that it is able to more accurately account for the heterogeneity effect in the cross sections.

The MC^2-3 code produces cross sections in the ISOTXS format which is readable by PROTEUS. In most cases, cross sections were generated for homogeneous assemblies rather than heterogeneous regions since the heterogeneity effect is not significant in fast reactors due to a long mean free path of fast neutrons.

Over the years, the cross sections generated from MC^2-3 have been verified and validated against many fast spectrum reactors and experiments. Verification and validation (V&V) tests against thermal systems have been in progress since the thermal cross section capability was implemented.

2.1.2 Using Monte Carlo Codes

Many Monte Carlo codes have a capability of generating multigroup cross sections, the quality of which has been improved with advanced methodologies so that those cross sections could be used for deterministic codes to some extent. As an alternative cross section generation option, we developed a utility code, named GenISOTXS, which is able to process the cross section output from Serpent and OpenMC Monte Carlo codes to produce a complete set of cross sections in the ISOTXS format.

The Serpent code mainly produces macroscopic cross sections, even though generating microscopic cross sections except for scattering matrices. The maximum number of cross section groups is limited to 70 groups and the group structures are fixed. Therefore, a smaller number of groups should be within the 70 group structure and the use of the multigroup cross sections may be limited.

On the other hand, the OpenMC code is able to produce microscopic cross sections and its Python API provides some flexibility of processing multigroup cross sections for users. Both Monte Carlo codes still have the limitation that the higher moments of multigroup scattering cross sections are generated by weighting with the 0^{th} moments of fluxes (scalar fluxes) instead of the higher moments of fluxes.

Using the Monte Carlo codes, homogeneous or heterogeneous region cross sections can be generated as a user wants. Those cross section outputs can be converted to the ISOTXS format using the GenISOTXS code. Verification tests were tested for several cases including the TREAT experiments. For TREAT, the 11-group macroscopic cross sections were tallied from many representative heterogeneous regions using Serpent. Those cross sections were used for a whole-core calculation with PROTEUS, producing accurate eigenvalue and power distributions in comparison with Serpent solutions [13]. In this process, however, the solution accuracy is dependent on how appropriately cross section groups and regions are selected.

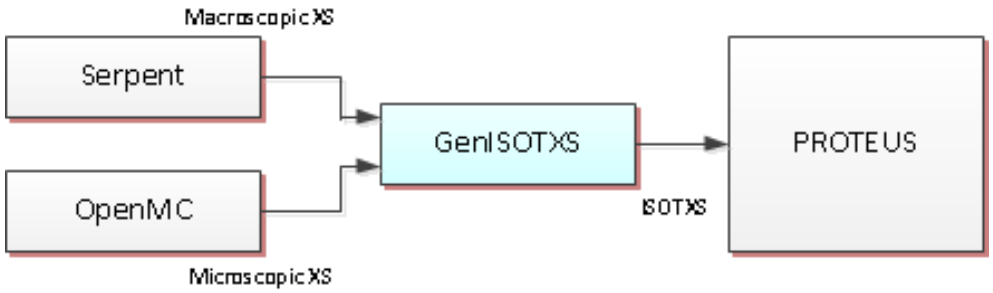

Figure 1. Use of Cross Sections Generated from Serpent and OpenMC for PROTEUS.

2.2 Multigroup Cross Sections Using the CSAPI

2.2.1 The Subgroup Method

In the subgroup method [5], the effective resonance cross sections for each group are represented with a combination of subgroup levels or cross sections (σ_{xn}), subgroup weights (w_{xn}), and subgroup scalar fluxes (ϕ_n) at the subgroup levels ($n = 1,...,N$) for each cross section type (x = absorption, nu-fission, and scattering), as shown below.

$$\sigma_x = \frac{\sum_N w_{xn}\sigma_{xn}\phi_n}{\sum_N w_{an}\phi_n}, \tag{1}$$

where the summation of the subgroup weights should be unity and $\phi_n = \sigma_{bn}/(\sigma_{an}+\sigma_{bn})$.

The subgroup fluxes are calculated by solving the fixed source equations, Eq. (2), for each group which are decoupled and thus can be solved in parallel. The background cross sections (σ_{bn}) are determined using the subgroup fluxes, based on Eq. (3). The subgroup parameters w_n for individual isotopes are prepared as a function of background cross section and temperature. The resonance interference effect due to the presence of other resonant isotopes in a mixture is accounted for using the Bondarenko iteration in which other isotope cross sections are treated as a constant over each energy group.

$$\hat{\Omega}\cdot\nabla\psi_n + (N_r\sigma_{an} + \sum_i \lambda_i\Sigma_{ip})\psi_n = \sum_i \lambda_i\Sigma_{ip}, \tag{2}$$

where N_r, Σ_p, and ψ_n denote the number density of the resonant nuclide, the potential cross section, and the angular flux, respectively. Equivalence theory enforces that the self-shielded scalar flux is expressed with the absorption (σ_{an}) and the background cross sections (σ_{bn}).

$$\sigma_{bn} = \frac{\sum_i N_i\lambda_i\sigma_{ip} + \Sigma_{en}}{N_r} = \frac{\sigma_{an}\phi_n}{1-\phi_n}. \tag{3}$$

The resonance integral (RI) can be calculated using the subgroup weights, levels and background cross sections as the following equation.

$$RI_x = \sum_n w_n\sigma_{xn}\frac{\sigma_{bn}}{\sigma_{an}+\sigma_{bn}}. \tag{4}$$

Once the RI values are determined using Eq. (4), the self-shield absorption, nu-fission, and scattering cross sections are estimated using the background cross section (σ_b) and the absorption, nu-fission, and scattering RIs as below.

$$\sigma_a(\sigma_b) = \frac{RI_a(\sigma_b)}{1-RI_a(\sigma_b)/\sigma_b}, \tag{5a}$$

$$\nu\sigma_f(\sigma_b) = \frac{RI_{nf}(\sigma_b)}{1 - RI_a(\sigma_b)/\sigma_b}, \tag{5b}$$

$$\sigma_s(\sigma_b) = \frac{R_s(\sigma_b)}{1 - RI_a(\sigma_b)/\sigma_b}, \tag{5c}$$

where σ_a is the absorption cross section, σ_f is the fission cross section, ν is the number of neutrons released from a fission, and RI_a, $RI_{\nu f}$, and RI_s are absorption, nu-fission, and scattering resonance integrals, respectively.

2.2.2 The Resonance Table Method

In the subgroup method being widely used for calculating the effective resonance cross sections, the fluxes and resonance integral are represented with subgroup parameters (levels and weights) in the quadrature form. The accuracy of the subgroup method relies on the accuracy of the subgroup parameters. The subgroup weights are determined using the least square approach to minimize the errors in the reconstructed effective cross sections compared to many heterogeneous pin cell reference solutions.

In the Dancoff approach based on equivalence theory [11], the multigroup resonance integral libraries can be simply generated with a homogeneous geometry problem using NJOY while the subgroup method requires to use a heterogeneous geometry problem to improve the accuracy in the actual calculations. Two-term or multi-term rational approximations should be introduced to improve the accuracy in estimating the effective cross sections of a heterogeneous geometry problem. Since the fuel lump is treated as black in the methodology, a special treatment is required to address the spatial self-shielding effect inside the fuel lump.

Both methods above require significant efforts and experiences in order to generate cross section parameters that ensure the accurate reproduction of the effective resonance cross sections for various background cross section and temperature conditions. The resonance table approach is simple and would be accurate if the background cross sections can be estimated for any heterogeneous geometry problems in consistent with the table that is generated based on a heterogeneous pin cell.

2.2.3 The Ultrafine Group-based Cross Section Library

The CSAPI of PROTEUS is able to deal with the cross section library based on the resonance table method. In this method, the base ultrafine group (UFG) cross section library is generated using MC^2-3 and NJOY. The library includes the resonance cross section tables for absorption, nu-fission, and scattering cross sections as a function of the background cross section and temperature for each isotope. The number of the background cross sections in the resonance table should be different depending upon isotopic characteristics. The UFG structure is composed of 2158 groups, including 2123 groups from 20 MeV to 0.414 eV, and 35 groups from 0.414 to 10^{-4} eV with variable lethargy intervals. Relatively large lethargies in the thermal energy range are assigned because there is no significant cross section variation as in the resonance energy range. We use MC^2-3 to obtain all cross section data above 0.414 eV and NJOY to collect thermal cross

section data below 0.414 eV and update scattering data below 3 eV. The resonance cross section tables are calculated using the hyperfine group (~600,000) slowing-down calculation option of MC^2-3. We checked that the ultrafine group resonance cross sections of major isotopes determined by the hyperfine group calculation of MC^2-3 agreed very well with MCNP6 solutions.

Preliminary verification tests indicate that the base UFG cross section library is able to accurately estimate eigenvalue and cross sections for various compositions with different characteristics. However, an UFG library has too many groups for practical use, so it is necessary to condense it to a practical number of groups. We use a group condensation optimization algorithm to condense an UFG library to a broad group (BG) library minimizing the loss in accuracy for a particular reactor type of interest. Once a reactor of interest is selected, the UFG slowing-down calculation is first performed with a representative homogeneous composition to determine the UFG neutron spectrum. Then, multiple homogeneous and heterogeneous compositions available for the specific core(s) are prepared to determine the BG boundaries which can best approximate the solutions with the UFG cross section library in terms of partial reaction rates (absorption and nu-fission) and eigenvalue.

2.2.4 The Broad Group Cross Section Library Using a Monte Carlo Code

In the method, unlike the ultrafine group-based cross section method, the reference multigroup cross sections are generated directly from a Monte Carlo code based on representative pin cell calculations. Those cross sections are correlated with the corresponding background cross sections derived from the deterministic code for each isotopes.

The OpenMC code is used for the reference microscopic cross section generation, and MC^2-3 with a 2-D MOC capability is employed for calculating the corresponding background cross sections. The method calculating the background cross sections taking into account the heterogeneous geometry effect is as follows.

Based on the collision probability method and the reciprocity theorem, the flux at region i in a heterogeneous geometry can be expressed as

$$\phi_i(u) = \frac{\sum_j P_{ji}(u) S_j(u) V_j}{\Sigma_{ti}(u) V_i} = \frac{\sum_j P_{ji}(u) S_j(u) V_j}{\sum_j P_{ji}(u) \Sigma_{tj}(u) V_j} \approx \frac{\sum_j P_{ji}(u) \Sigma_{pj} V_j}{\sum_j P_{ji}(u) \Sigma_{tj}(u) V_j}, \tag{6}$$

where $P_{ji}(u)$ is the collision probability from region j to i, $\Sigma_{tj}(u)$ and Σ_{pj} is the total and potential cross sections of region j, respectively, and V_j is the volume of region j. Using the Tone's approximation, the flux can be represented with the potential cross section based on the NR approximation. Eq. (6) can be rewritten for a resonant isotope as

$$\phi_i^r(u) = \frac{\sigma_{0pj}^r(u)}{\sigma_{aj}^r(u) + \sigma_{0tj}^r(u)}, \tag{7}$$

$$\sigma_{0tj}^r(u) = \frac{\sum_j \sum_{k \neq r} P_{ji}(u) \Sigma_{tj}^k(u) V_j}{\sum_j P_{ji}(u) N_j^i V_j}. \tag{8}$$

where the subscript 0 denotes the background cross section which includes the material background and escape cross sections.

The total background cross section, Eq. (8), is estimated using multi-group collision probabilities under the assumption $P_{ji}(u)/\Sigma_{ti}(u) = \alpha_i(u)P_{ji}/\Sigma_{ti}$, being rewritten with group constant quantities as

$$\sigma_{0ti}^{r} = \frac{\sum_j \sum_{k\neq r} P_{ji} N_j^k \sigma_{tj}^k V_j}{\sum_j P_{ji} N_j^r V_j}. \tag{9}$$

The escape cross section for a resonant isotope r at a region i can be defined as

$$\sigma_{ei}^{r} = \sigma_{0ti}^{r} - \sum_{k\neq r} \Sigma_{ti}^{r} / N_i^r. \tag{10}$$

Based upon the equation above, the escape cross section is an isotope- and region-dependent quantity. Eq. (9) can be solved by using the two fixed source problems with different sources for a resonant isotope r and each group

$$\Omega \cdot \nabla \psi_n^r(\mathbf{r},\Omega) + \Sigma_t(\mathbf{r})\psi_n^r(\mathbf{r},\Omega) = S_n^r(\mathbf{r}) \ (n=1,2), \tag{11}$$

where $S_1^r = \sum_{k\neq r} \Sigma_t^k(\mathbf{r})$ and $S_2^r = N^r(\mathbf{r})$. The total background cross section can be estimated by the ratio of the scalar flux solutions, ϕ_1^r / ϕ_2^r, which allows us to calculate it without knowing the collision probabilities and thus to use S_N or MOC instead. Since the total cross section including resonance cross sections are determined by the background cross section, the escape cross sections are calculated iteratively. However, the solutions are normally converged very quickly in 2-3 iterations.

The broader the energy group is, the less accurate the background cross sections estimated using the method above would be. However, it would not be a problem in this approach because the background cross section is not directly used for resonance cross section calculations but used as a parameter for the cross section tabulation.

3. Cross Section Library Generation for PROTEUS

3.1 Isotopic Cross Sections

The base isotopic cross sections with various background conditions for each isotope are generated from OpenMC Monte Carlo calculations using heterogeneous unit pin cells with the change of number density of the isotope of interest. In this calculation, it should be ensured that the change of number densities can cover all possible background cross section ranges from infinite dilute to almost pure self-shielding conditions.

The OpenMC code is an open-source Monte Carlo particle transport code capable of simulating 3-D models via constructive solid geometry, which has been developed and maintained as a community code with contributions from researchers at ANL, MIT, and various

others universities and laboratories. It is supported by the Python API that enables programmatic pre- and post-processing, thereby aiding users in generating and analyzing complex models.

The code provides a capability to perform both cross-section generation and flux calculations on a detailed 3-D geometry in continuous energy. In the last few years, the code have provided more input flexibility, improved computing efficiency, and better capability for tallying cross sections that are to be used with deterministic neutronics codes. The OpenMC code was recently developed with enhanced capability for cross-section (XS) generation, and the GenISOTXS code was developed at ANL to convert the XS output into the ISOTXS format for use in the ANL suite of neutronics codes.

The OpenMC code has the ability to generate isotope-wise microscopic cross-sections including scattering, (n,2n) and (n,3n) matrices over arbitrary spatial regions. Note that anisotropic scattering cross sections are weighted with the scalar fluxes instead of the higher moments in the same way as other Monte Carlo codes. In order to calculate microscopic cross sections for a given reaction over spatial regions with material heterogeneity, a stochastic volume calculation algorithm is used to provide estimates of average isotope densities over the region. While OpenMC implements several different tally estimators, an analog estimator was used for all tallies in this study in order to maintain consistent neutron balance.

A typical pin cell of LWR is selected for cross section calculations, whose geometry and compositions are shown in Figure 2 and Table 1, respectively. An air gap between pellet and cladding is removed for simplicity. For each isotope, its number densities are changed by multiplying 32 to 1/256 to its base number density in order to provide a wide range of background cross sections possible in the actual conditions. Currently, 14 cases are made with different number densities of the isotope of interest. OpenMC is then executed for those cases using 20 million particle histories, tallying all microscopic cross sections based on a given multigroup energy structure. Actinides and fission product isotopes are placed in the fuel region and other isotopes are put in the cladding or moderation region.

Conventionally, only resonances of the isotope of interest are considered in a pin cell calculation, using the potential cross sections for the other resonant isotopes, so that the effect of those resonances is separated out from those of the other resonance isotopes. In this procedure, the interference effect between resonant isotopes is ignored or additionally accounted for by introducing correlations between them. However, in this procedure, all resonances of isotopes are used in the calculations as they are.

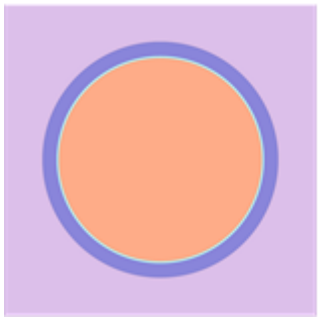

Figure 2. A Unit Pin Cell Used for Cross Section Generation with OpenMC

Table 1. Composition of the Unit Pin Cell.

Region	Composition [$\times 10^{24}$ #/cm^3]
Fuel	U-235 7.18132E-4 U-238 2.21546E-2 O-16 4.57642E-2
Cladding	ZR-90 4.25394E-2 FE-56 1.36306E-4
Moderator	O-16 2.48112E-2 H-1 4.96224E-2

3.2 Resonance Cross Sections

Once the microscopic cross sections of the isotope of interest are produced from OpenMC, the background cross sections corresponding to those cross sections are calculated using MC^2-3. The recently updated version of the MC^2-3 code includes a 2-D and 3-D MOC capabilities for Cartesian and hexagonal geometries. In the version, anisotropic scattering with up to P_3 can be handled with the 2-D MOC calculation. The escape cross sections for heterogeneous problems are calculated by solving the fixed source problems discussed in Section 2.2.2.

With the cross sections provided from OpenMC, one-group fixed source problems given in Eq. (11) are solved for all resonance energy groups of the isotope of interest. At every resonance energy group, data points (background cross sections) with the number of cases are generated, which would be all different between resonance energy groups.

Since a single set of background cross sections are needed for all resonance energy groups, a combined set of background cross section is generated by merging all background cross sections from all resonance energy groups, instead of selecting some data points from them, in order to reduce the errors arising from interpolation. The cross section tables are made for absorption, nu-fission, and total scattering cross sections as

$$\sigma_x = f(\sigma_b, T), \tag{12}$$

where the subscript x represents absorption, nu-fission, and scattering and σ_b is the background cross section.

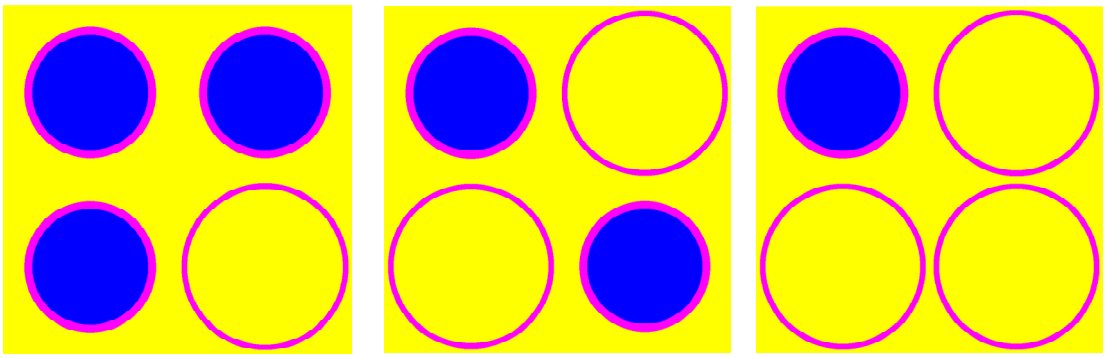

Figure 3. Four Different Combinations of Fuel Pins (Blue) and Guide Tubes (Yellow) for Calculating Self-shielded Cross Sections.

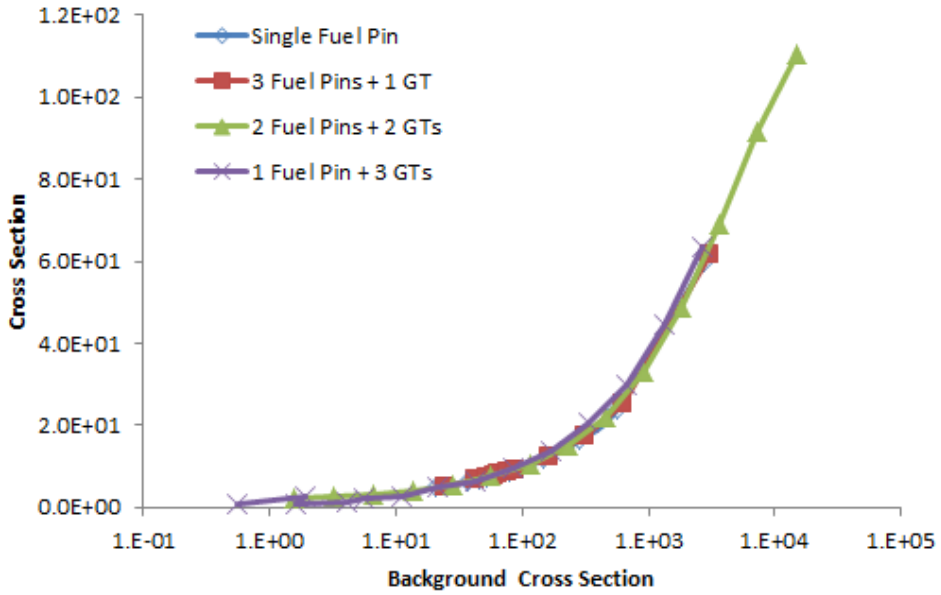

Figure 4. Absorption Cross Section versus Background Cross Section of U-238 at 4 – 9.88 eV Obtained from 4 Different Pin Configurations.

In this approach, it is necessary to check if the correlation of resonance cross sections and background cross sections prepared from pin cells with specific background cross section conditions can be applicable to other background cross section conditions. For the test, the cross section table generated with a pin cell was compared with those produced with three different 2×2 pin configurations: 1) 3 fuel pins + 1 guide tube (GT), 2) 2 fuel pins + 2 GTs, and 3) 1 fuel pin + 3 GTs. All cases have the same material background cross sections but very different escape cross sections. Nevertheless, comparisons indicated that the U-238 absorption cross sections at 4-9.9

eV from the three 2×2 pin calculations agreed well with those from a single pin cell, as shown in Figure 3. In fact, the three cases have very different neutron spectra due to the increased thermalization or absorption of neutrons in the different number of GT regions, which would affect the multigroup cross sections.

3.3 Cross Section Library

3.3.1 Flux Correction Factor

The angular dependency of resonance multigroup cross sections [14] may become more significant as the number of energy groups is reduced. This means that even though the multigroup cross sections tallied from the reference code are used, its multigroup flux solutions may not be reproduced in other deterministic codes unless the angular dependency of cross sections of the reference solution is preserved. Figure 5 shows the comparison of fluxes produced from OpenMC and MC^2-3 for the unit pin cell shown in Figure 2. Even though the 41-group cross sections tallied from OpenMC are used in MC^2-3, the flux solutions are different from each other in the resonance and thermal energy range, which makes eigenvalue off by more than 200 pcm.

In order to reproduce reaction rates, we introduce the flux correction factor, based on Eq. (7), which is calculated from MC^2-3 using the iterations until they are converged.

$$\mu_g(r) = \frac{\phi_g(r)}{\phi_g^{'}(r)}, \tag{13}$$

where $\phi_g(r)$ and $\phi_g^{'}(r)$ are the reference and calculated fluxes. The flux correction factors should vary with material and geometry conditions. However, we calculate the flux correction factors for the representative pin cell and apply them to the fuel region only, assuming that the fuel region is the most dominant contributor to determine neutron fluxes and eigenvalue. Verification tests that will be discussed in the next section indicated that the approximation works well for most of the benchmark problems.

Figure 6 illustrated the 41, 47, and 70-group structures tested. The 47-group and 70-group structures stem from the HELIOS and LANL group structures, respectively. Since the smaller number of groups is preferred for PROTEUS at the end and the 47-group structure was found to produce larger errors in eigenvalue estimation, the 41-group structure was proposed here maintaining almost the accuracy of the 70-group solutions. Figure 7 depicts the flux correction factors calculated from MC^2-3, showing that relatively large corrections are needed in the resonance and thermal energy range. Interestingly, it was found that a relatively large correction is necessary for the group of 6.48-7.34 eV for the 47-group structure where the largest capture resonance cross section of U-238 exists. The 47-group structure has finer groups in the range of 4 – 10 eV than the other two group structures.

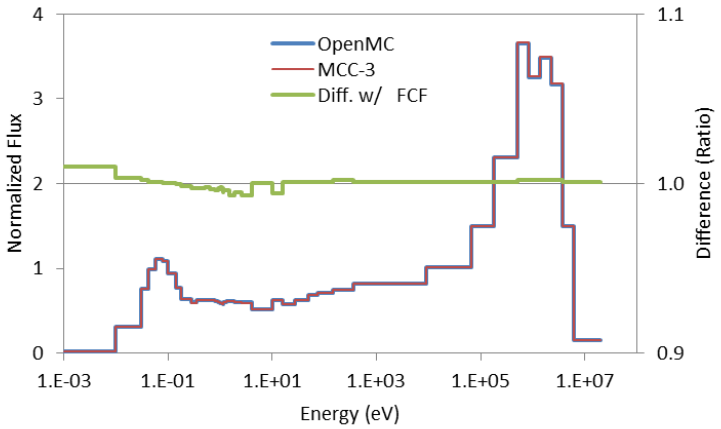

Fuel Region

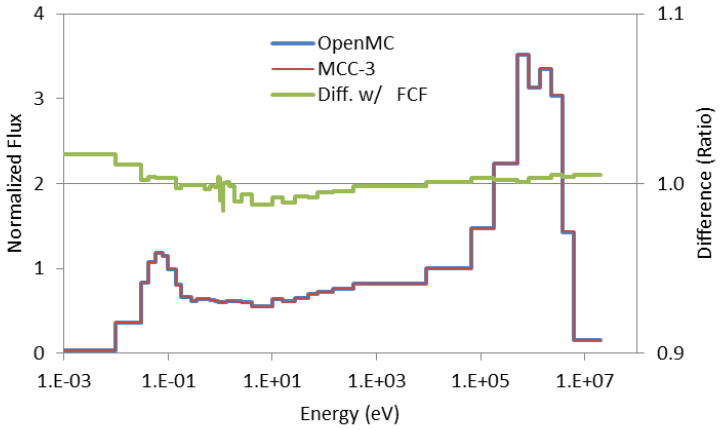

Cladding Region

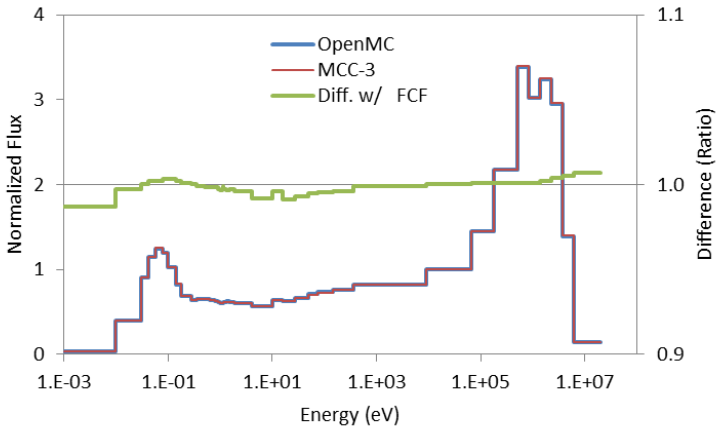

Moderator Region

Figure 5. Neutron Flux Differences between OpenMC and MC^2-3 for the Unit Pin Cell.

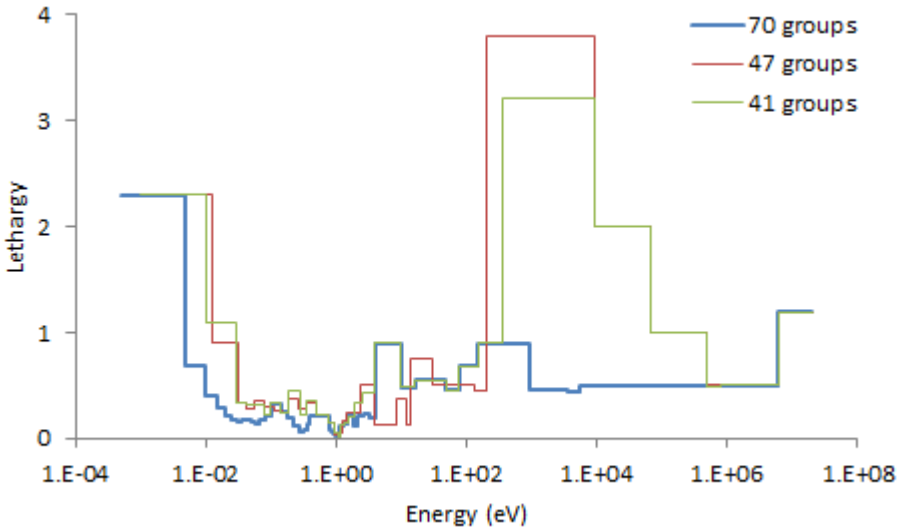

Figure 6. Energy Group Structures of the 41, 47, and 70-Group Cross Section Libraries.

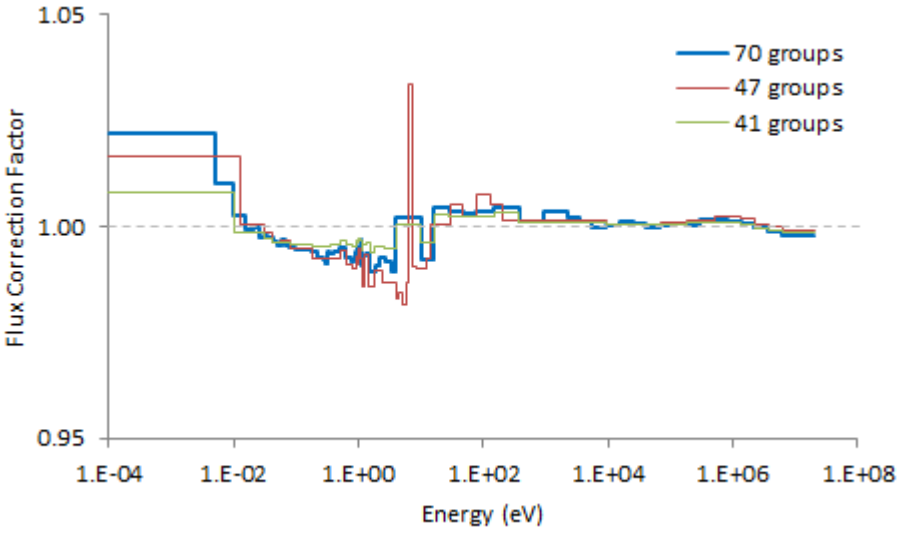

Figure 7. 41, 47, and 70-group Flux Correction Factors for the Fuel Region.

3.3.2 Library Generation

Once the isotopic cross sections and background cross sections are calculated for each isotope with a wide range of background cross sections and temperature conditions, the resonance cross sections for absorption, nu-fission, and total scattering are tabulated with background cross sections and temperatures, and the cross sections in the non-resonance groups as well as scattering matrices are extracted from the representative pin cell.

Total scattering cross sections contain all of elastic, inelastic, (n,2n), and (n,3n) cross sections in the production basis. (n,p), (n,d), (n,t), and (n,α) reaction cross sections are not available separately at the moment, which are included in the absorption cross section.

$$\sigma_a^{'} = \sigma_a - \sigma_{n2n} - 2\sigma_{n3n}, \tag{14}$$

$$\sigma_{tr} = \sigma_t - \sigma_{s1},$$

$$\sigma_s^{'} = \sigma_s + 2\sigma_{n2n} + 3\sigma_{n3n},$$

$$\sigma_{sgg'}^{'} = \sigma_{sgg'} + 2\sigma_{n2n,gg'} + 3\sigma_{n3n,gg'},$$

$$\sigma_t = \sigma_a^{'} + \sigma_s^{'} = \sigma_a + \sigma_s + \sigma_{n2n} + \sigma_{n3n},$$

where σ_t ,σ_{tr}, σ_a, and σ_s are the total, transport, absorption, scattering cross sections, $\sigma_{sgg'}$ is the scattering matrix from g to g', and σ_{s1} is the total P_1 scattering cross sections. The total cross section can be retrieved by adding $\sigma_a^{'}$ and $\sigma_s^{'}$ as in Eq. (14).

The CSAPI of PROTEUS reads the cross section library and solves the fixed source problems, given in Eq. (6), for each isotope and group to calculate the isotopic escape cross sections for all cross section regions. Varying with the background cross sections, the total cross sections used in the fixed source problems are iteratively determined but converged very quickly in 2 to 3 iterations. The final multigroup cross sections are determined by the total background cross sections composed of the escape cross sections and material background cross sections.

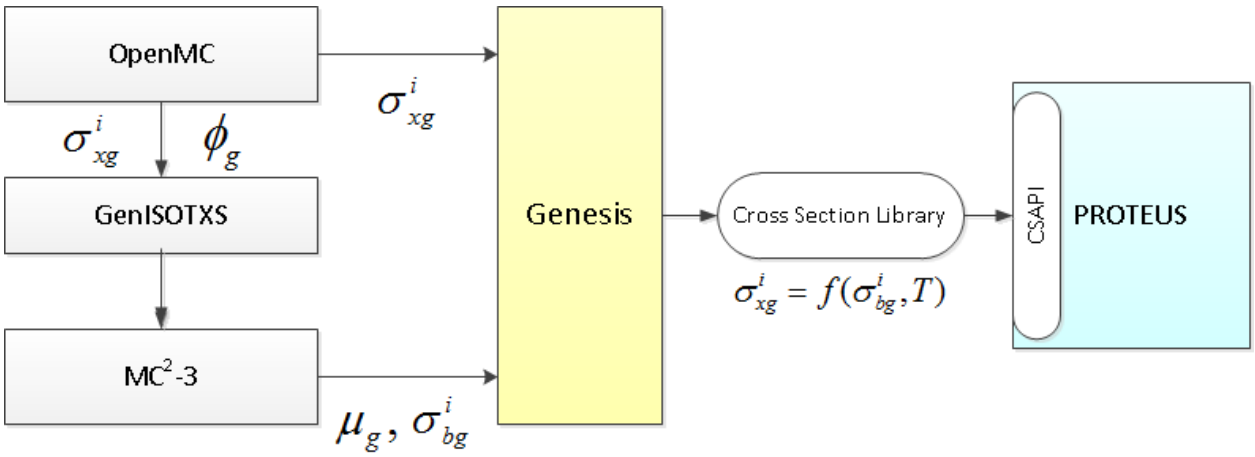

Figure 8. Generation of the Cross Section Library for PROTEUS.

The contribution of the updated resonance cross sections to the background cross sections for other isotopes is accounted for by the Bondarenko iteration. The resonance interference effect is not explicitly considered in the procedure, but the most part of the effect is included at the generation of cross sections with a pin cell. This would be a source of inaccuracy when the composition of the actual problem is very different from that of the representative pin cell. Figure 8 digests the flow from the cross section generation to the PROTEUS calculation.

4. Verification Tests

For verification of the cross section library generated based on ENDF/B-VII.0 data, multiple benchmark problems were selected including the Mosteller benchmark problems [15], the VERA fuel assembly benchmark problems [16], and the modified OECD/NEA C5 problems [17]. These benchmark problems were solved using PROTEUS-MOCEX with the 41-group cross section libraries whose solutions were compared against the corresponding Monte Carlo solutions. Hereafter, PROTEUS-MOCEX is referred to PROTEUS for brevity. Prior to testing the benchmark problems, a refinement study in terms of mesh, angle, and anisotropic scattering order was performed using a typical PWR pin cell to check a solution convergence. The in-house meshing tool named UFmesh [18] was used to create meshes for this study.

Due to a large computation time of PROTEUS, an attempt was made to reduce the number of groups maintaining the target accuracy. Thus, reviewing the HELIOS 47-group and LANL 70 group structure, we started with the 41-group structure which is similar to the 47-group structure. Compared to the 47-group structure, the 41-group structure has a little finer energy groups at 10 keV and a little coarser energy groups around 1 eV.

Preliminary calculations for the UO_2 pin cell using the three energy groups indicated that the 47 group structure increased the discrepancy of larger than 100 pcm between the deterministic and OpenMC solutions in eigenvalue and rather that the 41-group structure resulted in the solutions similar to the 70 group structure. More verification tests should be performed to make a conclusion. For the time being, test calculations were primarily done using the 41-group structure and more calculations will be followed with the 47-group and 70-group structures. A group optimization study will be conducted later on as well.

In addition, Table 2 indicates the characteristics of anisotropic scattering effect of UO_2 and MOX fuels. As known, the anisotropic effect (the difference between P_1 and P_2) is as large as 269 pcm in the MOX pin cell, while it is 61 pcm in the UO_2 pin cell. Normally, eigenvalue increases with the higher-order scattering, but it rather decrease here because it seems that the high-order scattering cross sections generated from OpenMC are inaccurate since they are weighted by scalar fluxes instead of higher-order moments. As noted in the previous section, the eigenvalues of the UO_2 and MOX pin cells were 212 pcm and 128 pcm off (based on the P_2 solutions from the 41 group structure) from the corresponding OpenMC solutions even though the multigroup cross sections generated from OpenMC were used.

Table 2. Eigenvalues from OpenMC and MC²-3 for the UO_2 and MOX Pin Cell Problems.

	Energy Group	Scattering	UO_2	MOX
OpenMC			1.36599 ± 0.00021	1.15961 ± 0.00021
			Δk, pcm	
MC²-3	41	P1	-273	-397
		P2	-205	-115
		P3	-212	-128
	47	P2	-332	
	70	P2	-202	

A mesh refinement study indicated that 3, 1, 1, and 2 annual rings were needed for fuel, gap, cladding, and moderator regions for a pin, respectively, as shown in Figure 9. For angles, a Legendre-Tchebychev angular cubature of $L_{13}T_{25}$, which is equivalent to 728 angular directions over 4π, was necessary to obtain a converged solution, as indicated in Table 2. For anisotropic scattering, it was found that a scattering order of P_2 is required because the differences between P_1 and P_2 results are 68 pcm for a UO2 pin and 282 pcm for a MOX pin and a minor impact is made by P_3 on both fuel types.

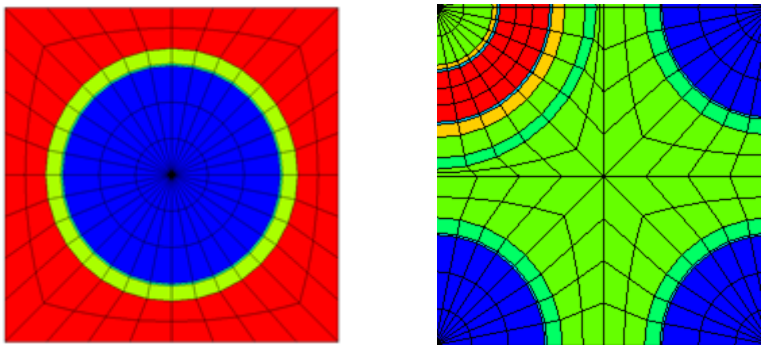

Figure 9. Meshes for a Single Pin or Multi-pins with a Burnable Absorber.

First, the Mosteller pin cell benchmark problems were used for verification tests, which include U or Pu enriched fuels with 0.71 to 5 wt.% U-235 (Cases 1 to 7) and 1 to 8 wt.% Pu-total (Cases 8 to 16). Among the MOX pins, Cases 8 to 12 contain reactor grade plutonium (60 wt.% Pu-fissile) while Cases 13 to 16 are composed of weapon grade plutonium (94 wt.% Pu-fissile). Eigenvalues from PROTEUS were compared with OpenMC solutions, indicating good agreement within 100 pcm Δk. No particular trend in eigenvalue differences between PROTEUS and OpenMC was observed with the change of enrichment. The detailed comparisons are listed in Table 5.

Table 3. Compositions of the UO2 and MOX Pin Cell Problems.

Region	UO2[a)]	MOX[b)]
Fuel	U-235 7.18132E-04 U-238 2.21546E-02 O-16 4.57642E-02	Pu-239 2.29802E-02 Pu-240 4.87043E-04 Pu-241 2.21051E-04 Pu-242 1.44567E-04 U-235 7.18132E-05 U-238 2.21546E-02 O-16 4.57642E-02
Cladding	Zr-90 4.25394E-02 Fe-56 1.36306E-04	Zr-90 4.25394E-02 Fe-56 1.36306E-04
Moderator	O-16 2.48112E-02 H-1 4.96224E-02	O-16 2.48112E-02 H-1 4.96224E-02

a) 3.1 wt.% U-235, b) 6.6 wt.% Pu-total

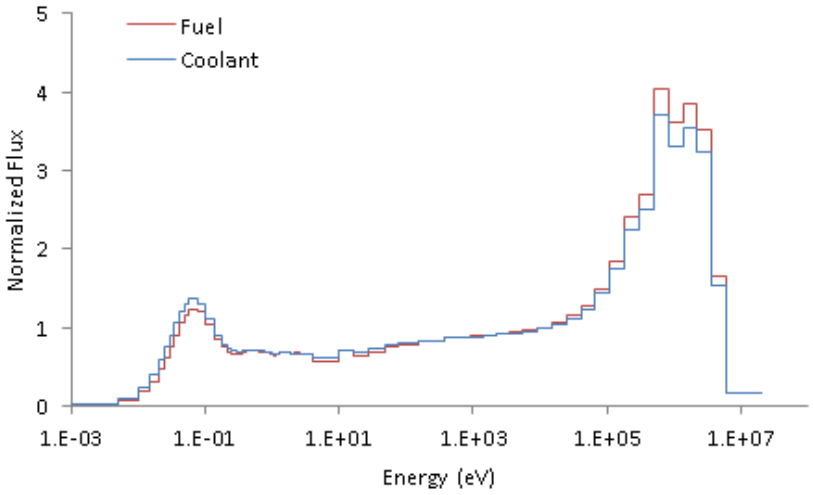

Figure 10. Normalized Flux Spectrum of a Typical LWR Pin Cell.

Table 4. Convergence of PROTEUS Solutions with Angular Orders for UO_2 Pin Cell Problem.

Polar [a)] \ Azimuthal [b)]	T15	T19	T25	T31
L5	1.36403	1.36404	1.36422	1.36417
L9	1.36424	1.36426	1.36446	
L13	1.36435	1.36434	1.36454	
L15	1.36436			

a) Legendre, b) Tchebychev angular cubature order

Table 5. Eigenvalue Comparison for the Mosteller Benchmark Problems.

Case	Enrichment U-235 / Pu-total, wt.%	OpenMC ±σ, pcm	PROTEUS Δk, pcm
1	0.71 / 0.00	0.68272 ± 14	-46
2	1.60 / 0.00	0.97821 ± 20	6
3	2.40 / 0.00	1.11598 ± 19	13
4	3.10 / 0.00	1.19319 ± 21	39
5	3.90 / 0.00	1.25525 ± 21	35
6	4.50 / 0.00	1.29063 ± 20	14
7	5.00 / 0.00	1.32427 ± 21	66
8	0.71 / 1.00 [a)]	0.93533 ± 19	-68
9	0.71 / 2.00	1.02184 ± 19	-74
10	0.71 / 4.00	1.08810 ± 21	8
11	0.71 / 6.00	1.12070 ± 20	-37
12	0.71 / 8.00	1.14595 ± 19	6
13	0.71 / 1.00 [b)]	1.08649 ± 20	-4
14	0.71 / 2.00	1.19280 ± 20	100
15	0.71 / 4.00	1.27192 ± 21	87
16	0.71 / 6.00	1.31047 ± 21	69

a) 59.9 wt.% Pu-fissile (rector grade Pu), b) 94.0 wt.% Pu-fissile (weapon grade Pu)

Before testing the VERA benchmark problems, the 2×2 pin problems were devised and solved by replacing a fuel pin with burnable poison, gadolinia pin, GT, control rod, and IFBA pin, as shown in Figure 11. The eigenvalue results are also compared in Table 6, showing that PROTEUS results are maximum 173 pcm Δk off from the OpenMC solutions.

For verification tests of fuel assemblies, the selected VERA PWR benchmark problems developed by the DOE CASL program based on the Westinghouse fuel were used as well. For simplicity, the original benchmark problems were slightly modified by simplifying compositions and using a constant temperature of 300K for all regions, resulting in different eigenvalues from the original ones. Case 2A is a standard fuel assembly (FA) with 264 3.1 wt.% U-235 enriched fuel pins, 24 guide tubes (GTs) and 1 instrument thimble (IT). The other six FAs include pyrex-type or WABA-type burnable poisons, AgInCd control rods, or IFBA. The calculation results indicated that the eigenvalues from PROTEUS agreed very well with MCNP6 solutions within 76 pcm Δk and the pin powers between the two codes had excellent agreement with 0.39%, except for Case 2P with 24 gadolinia (Gd) pins which showed a maximum difference of 2.05% at one of the Gd locations with 0.244 relative power. Excluding the Gd pins, the maximum and RMS differences of Case 2P are 0.43% and 0.17%, respectively, which are similar to the other cases. No particularly large differences were observed for Cases 2M and 2N with IFBA rods. Thermal flux, relative power, and % power differences for Cases 2G (with 24 CRs) and 2P (with 24 Gds) were illustrated in Figure 13. The results are digested in Table 7.

Multi-assembly calculations were performed for verification tests, which were created by modifying the OECD/NEA C5G7 benchmark problems. In the modification, a pin is composed of fuel, gap, cladding, and moderator regions, and isotopic compositions are used for the fuel regions: standard UO_2 (3.1 wt.% U-235) and MOX (enrichment zoning with 3.8, 6.6, and 7.4 wt.% Pu-total).

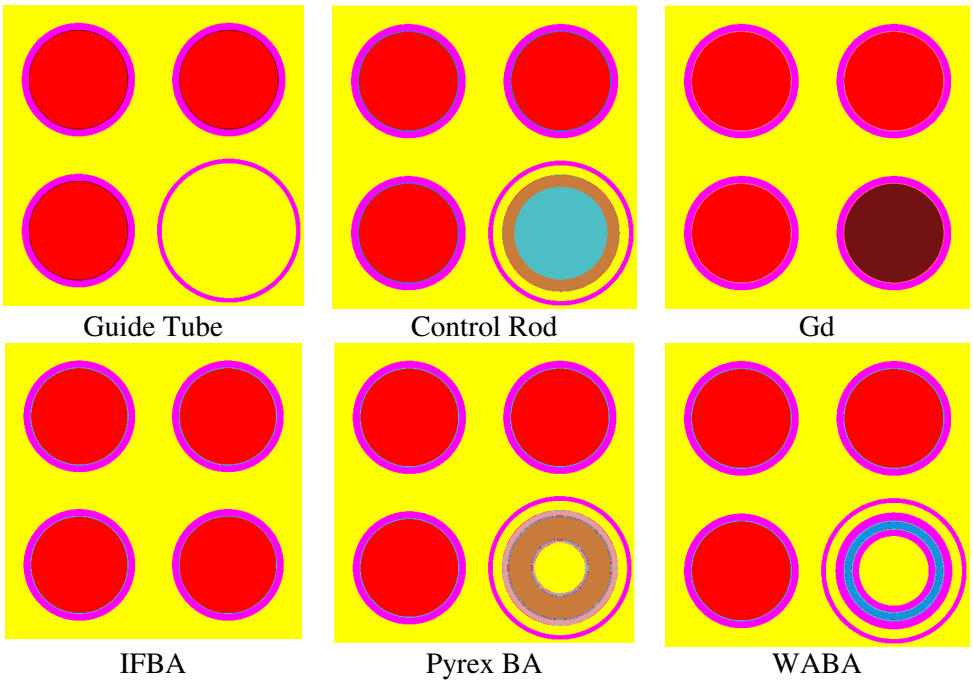

Figure 11. 2×2 Pin Benchmark Problems with GT, CR, Gd, IFBA, Pyrex BA, or WABA.

In this study, 2-D cores as well as FAs were calculated using PROTEUS and MCNP6. As expected from the previous comparisons for the VERA benchmark problems, FA eigenvalues and pin powers from PROTEUS agreed very well with MCNP6 solutions: eigenvalues within 52 pcm Δk and pin powers within 0.28% with RMS 0.16%, as illustrated in Figure 14.

For 2-D core problems, a base C5 case without CR was first solved using the two codes. For more challenging flux shapes and relatively flatter power distributions, an additional case was created by inserting 24 AgInCd CRs in the four UO_2 FAs located at the core center where relative powers in the case without CRs are up to 2.23. Flux and power distributions of the two cases are illustrated in Figure 15.

Compared to MCNP6 solutions, eigenvalues from PROTEUS are in good agreement within 141 pcm Δk and the control rod worths from the two codes matched well within 0.1%. A pin power comparison indicated that for the case without CR, maximum and RMS differences are 2.28% and 0.48%, respectively. In fact, the maximum percent difference occurred at the low power location of 0.33. If excluding the pins with less than a relative power of 0.5, the maximum and RMS differences are reduced to 1.41% and 0.43%, respectively. For the case with CRs, the

maximum and RMS differences in relative pin powers between the two codes are 1.45% and 0.53%, respectively. Its maximum difference is smaller than that of the case without CRs because the smallest relative power is as higher as 0.63 but the RMS of % differences is higher because of lager differences in the rodded UO_2 FAs.

Eigenvalue changes with temperature were tested using the selected VERA fuel assemblies: 2A, 2F, and 2G. Fuel temperatures were changed gradually from 300 to 1,200 K, maintaining the temperatures of the other regions with 300 K or 600 K, as shown in Table 9. MCNP6 calculations were performed using 25 million particle histories.

As shown in Table 9 and Figure 16, the eigenvalue solutions between MCNP6 and PROTEUS agreed well for most cases except Case 2G in which eigenvalues were off by up to 321 pcm. It is noted that only Case 2G includes 24 AgInCd control rods. An investigation will be performed for Case 2G to identify reasons and anything to make an improvement.

Table 6. Eigenvalue Comparison for the 2×2 Pin Benchmark Problems.

Case	3 Fuel Pins plus	OpenMC ±σ, pcm	PROTEUS Δk, pcm
1	Fuel	1.37182 ± 18	54
2	Guide Tube	1.41442 ± 19	-36
3	AgInCd CR	0.60051 ± 16	-46
4	Gd	0.80074 ± 17	-173
5	IFBA	1.19912 ± 17	82
6	Pyrex	0.79050 ± 17	-99
7	WABA	0.80097 ± 17	-119

Table 7. Eigenvalue and Power Comparison for the VERA Fuel Assembly Benchmark Problems.

Case	Description	MCNP6 ±σ, pcm	PROTEUS	
			Eigenvalue Δk, pcm	Pin Power Diff. Max / RMS, %
2A	3.1 wt.% Fuel	1.20546 ± 13	76	0.34 / 0.16
2F	+ 24 Pyrex BA	1.00796 ± 13	-3	0.39 / 0.18
2G	+ 24 AgInCd CR	0.90467 ± 13	7	0.35 / 0.15
2K	+ 24 Pyrex BA, 28 3.6 wt.% Fuel	1.05108 ± 13	-5	0.26 / 0.13
2M	+ 128 IFBA	0.95933 ± 12	-69	0.39 / 0.16
2N	+ 104 IFBA, 20 WABA	0.89635 ± 13	40	0.38 / 0.18
2P	+ 24 Gd	0.96792 ± 14	-39	2.05 / 0.60

* BA: Burnable Absorber, CR: Control Rod

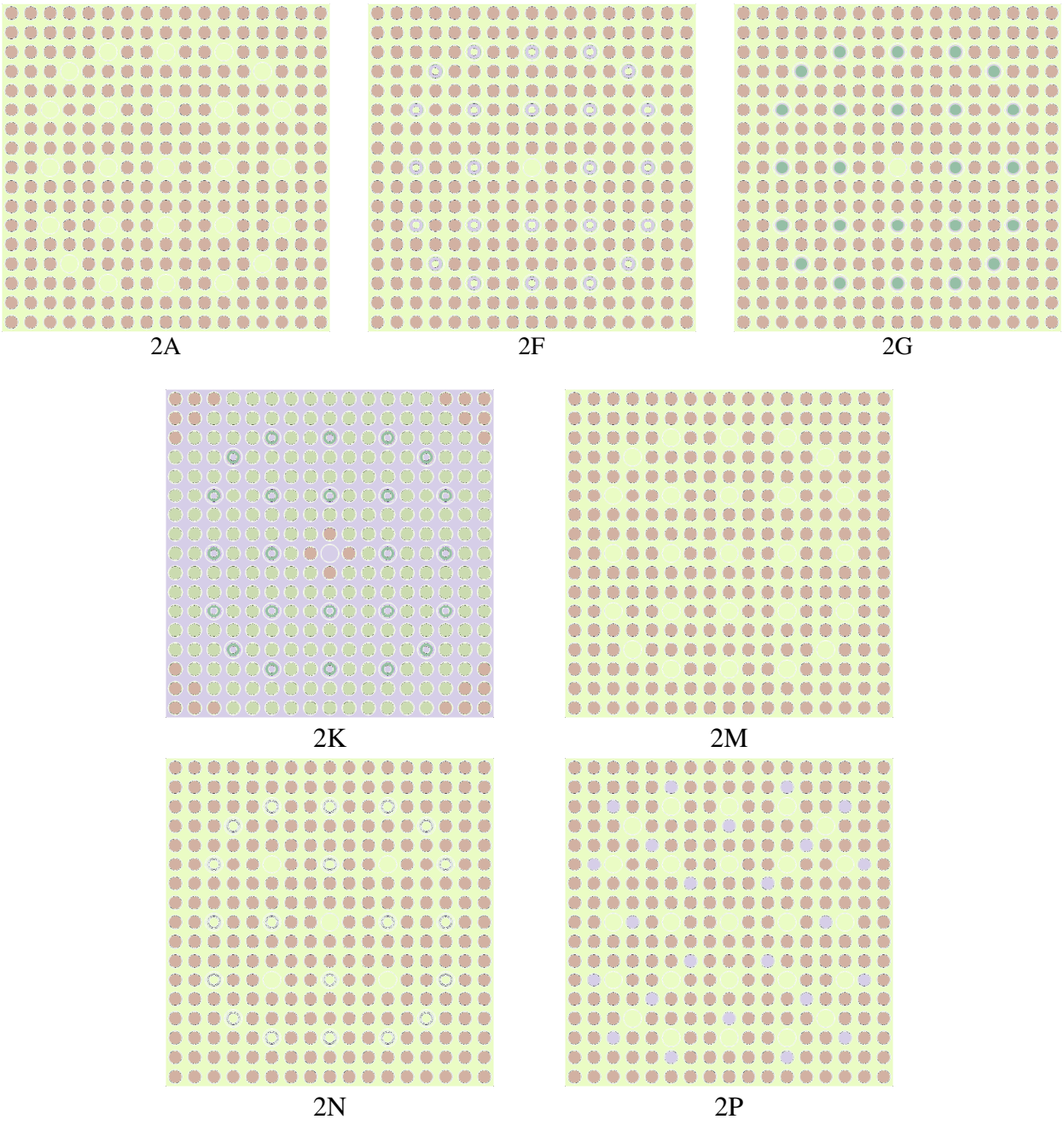

Figure 12. Fuel Assemblies Selected from the VERA Benchmark Problems.

Table 8. Eigenvalue and Power Comparison for the Modified C5 Benchmark Problems.

Case	MCNP6 ±σ, pcm	PROTEUS	
		Eigenvalue Δk, pcm	Pin Power Diff. Max/RMS, %
UO_2 FA	1.39208 ±17	-52	0.28 / 0.10
MOX FA	1.20450 ±12	12	0.29 / 0.16
2-D Core	1.19774 ±2	121	2.28 / 0.48
2-D Core w/ CR	1.04505 ±2	141	1.45 / 0.53
CR worth	15,269 (pcm)	-20 (0.1%)	

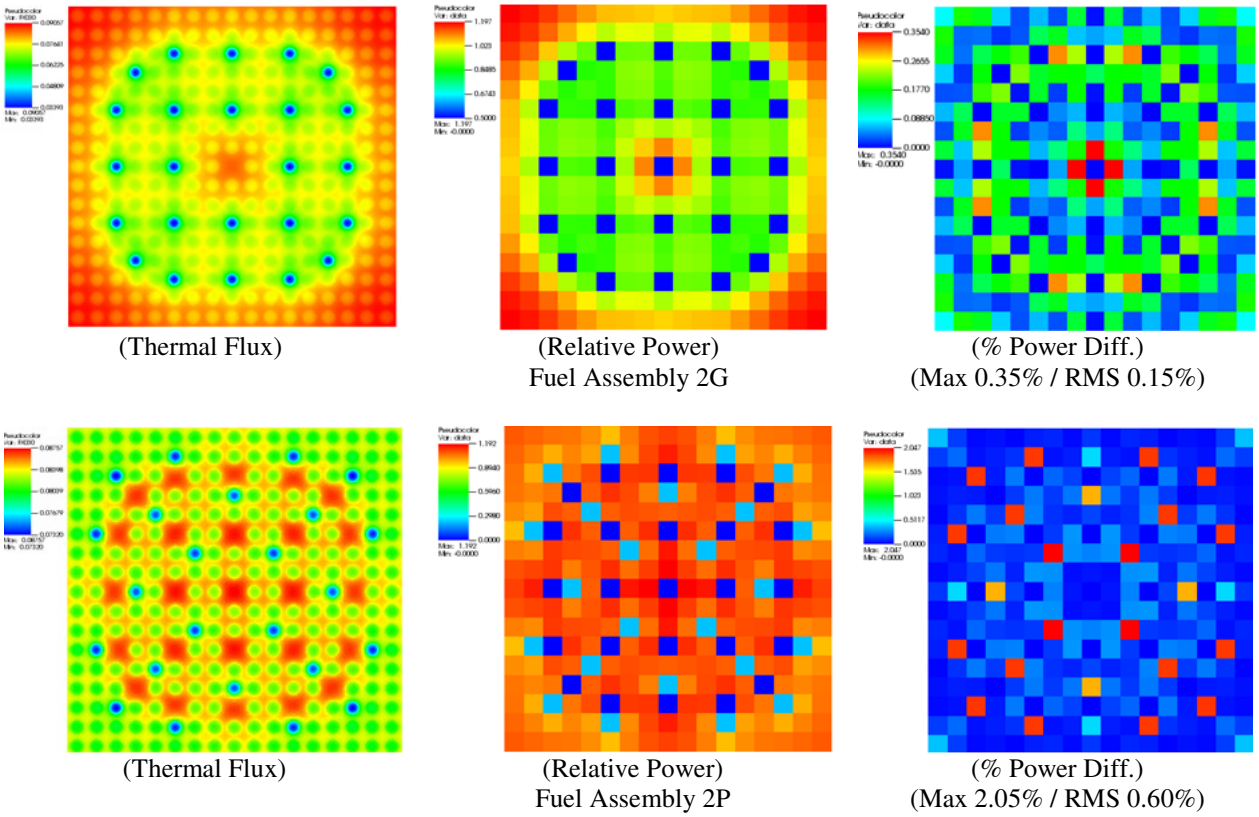

(Thermal Flux) (Relative Power) Fuel Assembly 2G (% Power Diff.) (Max 0.35% / RMS 0.15%)

(Thermal Flux) (Relative Power) Fuel Assembly 2P (% Power Diff.) (Max 2.05% / RMS 0.60%)

Figure 13. Thermal Flux, Relative Pin Power, and % Pin Power Difference of the VERA 2G and 2P Benchmark Problems.

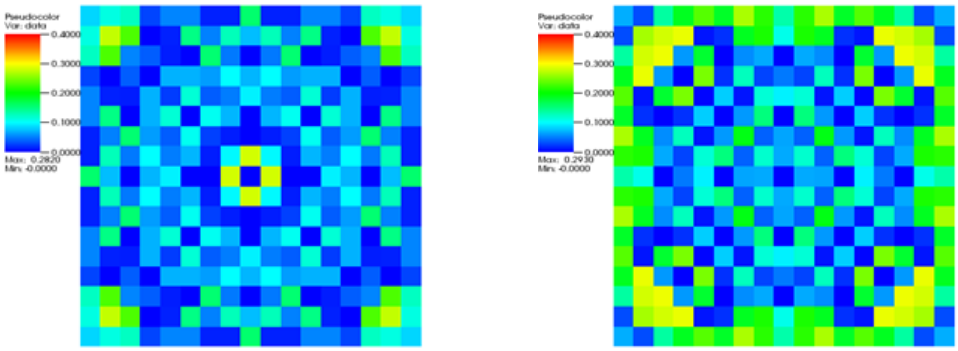

Max 0.28% / RMS 0.10% Max 0.29% / RMS 0.16%

Figure 14. Pin Power Difference of the UO_2 (left) and MOX (right) Fuel Assemblies of the C5 Benchmark Problems.

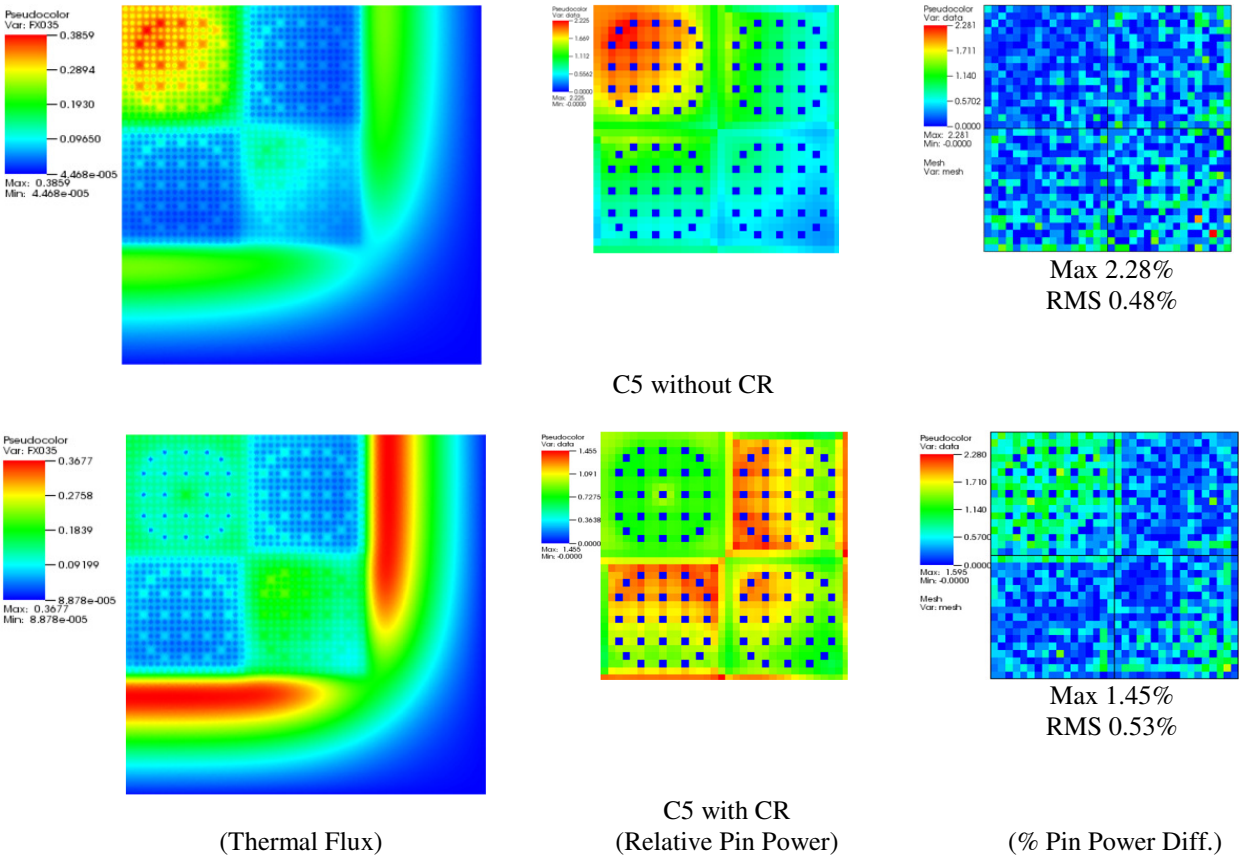

Max 2.28%
RMS 0.48%

C5 without CR

Max 1.45%
RMS 0.53%

C5 with CR
(Relative Pin Power)

(Thermal Flux)

(% Pin Power Diff.)

Figure 15. Thermal Flux, Relative Pin Power, and % Pin Power Difference of the 2-D C5 Benchmark Problems.

Table 9. Comparison of Eignvalues with Temperature Change between MCNP6 and PROTEUS for the Selected VERA Assemblies.

Case	Temperature Fuel / Other Regions (K)	MCNP6 $\pm\sigma$, pcm	PROTEUS Δk, pcm
2A	300 / 300	1.20546 ± 13	76
	600 / 600	1.19341 ± 13	198
	900 / 600	1.18467 ± 13	108
	1200 / 600	1.17693 ± 13	139
2F	300 / 300	1.00796 ± 13	-3
	600 / 600	0.98286 ± 13	52
	900 / 600	0.97565 ± 13	-52
	1200 / 600	0.96966 ± 13	13
2G	300 / 300	0.90467 ± 13	7
	600 / 600	0.87550 ± 13	-226
	900 / 600	0.86925 ± 13	-321
	1200 / 600	0.86410 ± 13	-259
2K	300 / 300	1.05108 ± 13	-5
	600 / 600	1.02748 ± 14	50
	900 / 600	1.02008 ± 13	-71
	1200 / 600	1.01356 ± 13	-69
2M	300 / 300	0.95933 ± 12	-67
	600 / 600	0.94709 ± 13	-23
	900 / 600	0.94051 ± 12	-109
	1200 / 600	0.93472 ± 12	-110
2N	300 / 300	0.89635 ± 13	40
	600 / 600	0.87664 ± 12	60
	900 / 600	0.87020 ± 12	-4
	1200 / 600	0.86512 ± 12	-49
2P	300 / 300	0.96792 ± 14	-39
	600 / 600	0.93559 ± 12	-37
	900 / 600	0.92899 ± 12	-135
	1200 / 600	0.92336 ± 12	-163

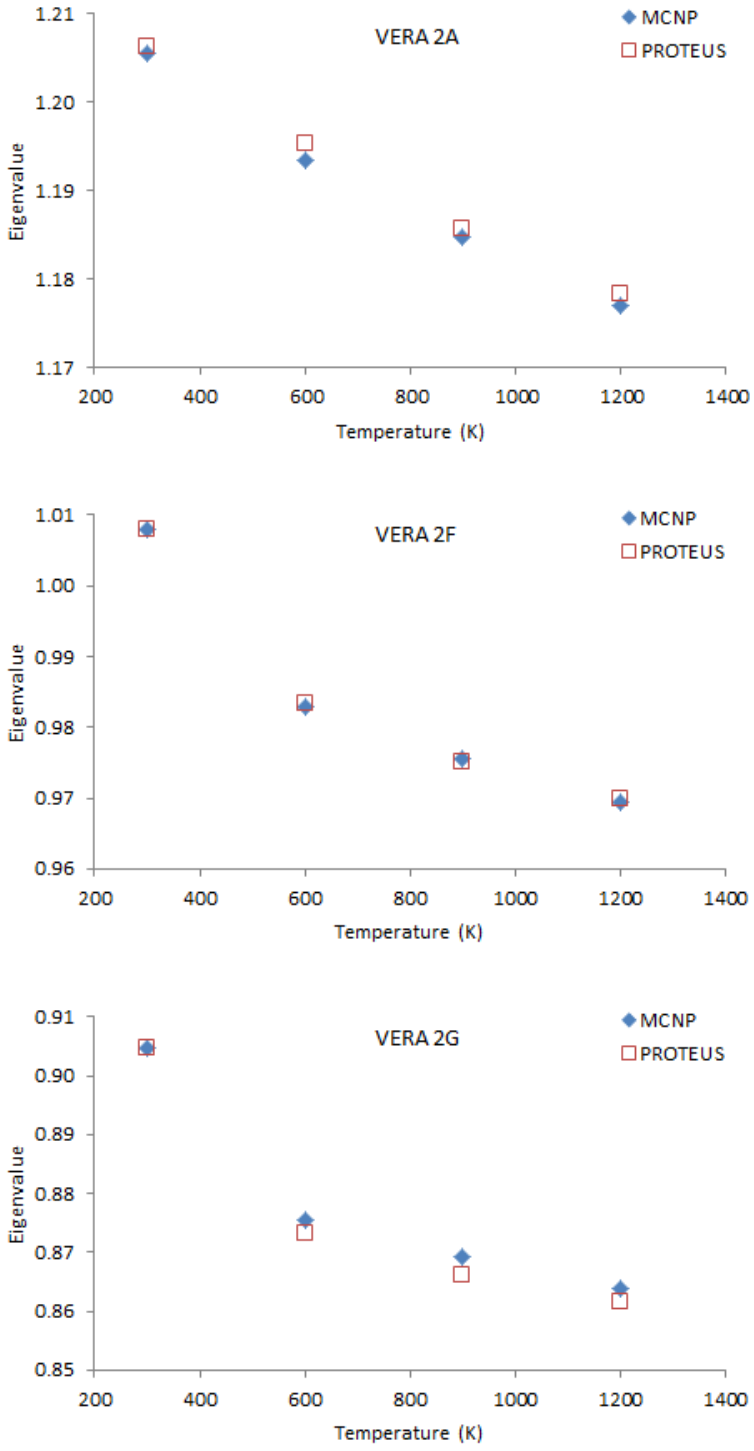

Figure 16. Eigenvalues with Temperature Change for the Selected VERA Assemblies

5. Conclusions

The PROTEUS code is able to read multigroup cross sections in the ISOTXS format provided offline using cross section generation codes or can generate multigroup cross sections on the fly using the cross section library which includes isotropic cross sections and resonance parameters as a function of temperature and background cross sections. For the latter, the cross section application programing interface (CSAPI) was available to make it easy to plug the cross section module into an existing neutron transport code. The CSAPI includes two cross section method options: the subgroup method and the resonance table method, both of which require the fixed source calculations at each energy group.

The subgroup method used for PROTEUS is consistent with the method used in the DeCART and HELIOS codes, while the resonance table method includes resonance cross sections tabulated as a function of temperature and background cross sections. For the resonance table method option, the base cross section library in the ultrafine group structure was generated using the hyperfine group calculations with MC^2-3 and thermal energy group cross sections from NJOY, which was then condensed to the based cross section library. The cross section library generation process for the resonance table method option has been recently updated with the broad-group based cross sections directly generated from the OpenMC Monte Carlo code to reduce errors in unit pin cell cross sections.

The new cross section library was generated based on the 41-group structure using OpenMC and MC^2-3 for use in PROTEUS, in which the isotopic cross sections including resonance cross sections were generated using OpenMC for a pin cell representing a reactor or reactor type of interest and the corresponding background cross sections were calculated using MC^2-3. The flux correction factors were also calculated from MC^2-3 in order to preserve reference reaction rates in the fuel region.

Verification tests of the 41-group cross section library were performed using the Mosteller pin benchmark problems, the selected VERA fuel assembly benchmark problems, and the modified OECD/NEA C5 benchmark problems. The test results indicated that PROTEUS was able to estimate eigenvalues very well within 100 pcm in most cases, compared with the OpenMC and MCNP6 Monte Carlo solutions. The pin powers from PROTEUS agreed very well with MCNP6 within 0.4% for most of the VERA fuel assembly cases and 2% for the modified C5 small core benchmark problems.

Based on the preliminary verification test results, it can be concluded that the new cross section library generated using OpenMC and MC^2-3 works well in solving LWR problems with PROTEUS. Further verification tests are planned for larger-size problems with more complex configurations. In addition, cross section libraries are being generated for other reactor types such as TREAT and MSR and verification tests of those cross section libraries will be performed as well.

References

1. E. R. Shemon, M. A. Smith, and C. H. Lee, "PROTEUS-SN Methodology Manual," ANL/NE-14/5, Argonne National Laboratory, June 30, 2014.
2. A. Marin-Laflech, M. A. Smith, and C. H. Lee, "PROTEUS-MOC: A 3-D Deterministic Solver Incorporating 2-D Method OF Characteristics," M&C, Sun Valley, ID, May 5-9, 2013
3. A. SIEGEL, et al, "Software Design of SHARP," *Proc. of M&C+SNA 2007,* 2007.
4. C. H. Lee, A. Marin-Laflache, and M. A. Smith, "Development of Cross Section Library and Application Programming Interface (API)," ANL/NE-13/15, Argonne National Laboratory, September 30, 2013.
5. HELIOS Methods, Studsvik Scandpower, November 20, 2003.
6. C. H. Lee and Y. S. Yang, "MC^2-3: Multigroup Cross Section Generation Code for Fast Reactor Analysis," *Nucl. Sci. Eng*., **187**, 268-290, June 2017.
7. R. E. MacFarlane, "NJOY 99/2001: New Capabilities in Data Processing," Presentation at the Workshop on Reactor Physics and Analysis Capabilities for Generation IV Nuclear Energy Systems, Argonne National Laboratory, Argonne, Illinois, February 18-19, 2003.
8. P. K. Romano et al., "OpenMC: A State-of-the-Art Monte Carlo Code for Research and Development," *Ann. Nucl. Energy*, **82**, 90, 2015.
9. N. E. Staff, P. K. Romano, C. H. Lee, and T. K. Kim, "Verification of Mixed Stochastic/Deterministic Approach for Fast and Thermal Reactor Analysis," ICAPP 2017, Fukui and Kyoto, Japan, April 24-27, 2017.
10. J. LEPPANEN, "Serpent – a Continuous-energy Monte Carlo Reactor Physics Burnup Calculation Code," VTT Technical Research Centre of Finland, June 18, 2015.
11. S. Y. Choi, C. H. Lee, and D. J. Lee, "Resonance Treatment Using Pin-based Pointwise Slowing-down Method," *J. Comp. Phys.*, **330**, 134-155, 2017.
12. B. K. Jeon, W. S. Yang, Y. S. Jung, and C. H. Lee, "Extension for Generation of Multigroup Cross Sections in Thermal Energy Range," M&C, Jeju, Korea, April 16-20, 2017.
13. C. H. Lee, Y. S. Jung, H. M. Connaway and T. A. Taiwo, "Simulation of TREAT Cores Using High-fidelity Neutronics Code PROTEUS," M&C, Jeju, Korea, April 16-20, 2017.
14. R. N. Hill, K. O. Ott, and J. D. Rhodes, "Directional Effects in Transitional Resonance Spectra and Group Constants," *Nucl. Sci. Eng*., **103**, 25-36,1989.
15. R. D. Mosteller, "The Doppler-defect Benchmark: Overview and Summary of Results," *Proceedings of M&C 2007*, Monterey, CA, April 15-19, 2007.
16. A. T. Godfrey, "VERA Core Physics Benchmark Progression Problem Specification," CASL-U-2012-0131-001, Rev.1, December 21, 2012.
17. M. A. Smith, E. E. Lewis, and B. C. Na, "Benchmark on Deterministic Transport Calculations without Spatial Homogenization: MOX Fuel Assembly 3-D Extension Case," OECD/NEA, NEA/NSC/DOC(2005)16, 2005.
18. M. A. Smith and E. R. Shemon, "User Manual for the PROTEUS Mesh Tools," ANL/NE-15/17 (Rev.2), Argonne National Laboratory, August 2016.

Nuclear Engineering Division
Argonne National Laboratory
9700 South Cass Avenue, Bldg. 208
Argonne, IL 60439-4842

www.anl.gov

Argonne National Laboratory is a U.S. Department of Energy
laboratory managed by UChicago Argonne, LLC